Quasielastic neutron scattering and molecular dynamics simulation studies of the melting transition in butane and hexane monolayers adsorbed on graphite

K. W. Herwig, Z. Wu, P. Dai,[a)] and H. Taub
Department of Physics and Astronomy and University of Missouri Research Reactor Facility,
University of Missouri—Columbia, Columbia, Missouri 65211

Flemming Y. Hansen
Department of Chemistry, Technical University of Denmark, IK 207 DTU, DK-2800 Lyngby, Denmark

Quasielastic neutron scattering experiments and molecular dynamics (MD) simulations have been used to investigate molecular diffusive motion near the melting transition of monolayers of flexible rod-shaped molecules. The experiments were conducted on butane and hexane monolayers adsorbed on an exfoliated graphite substrate. For butane, quasielastic scattering broader than the experimental energy resolution width of 70 μeV appears abruptly at the monolayer melting point of T_m = 116 K, whereas, for the hexane monolayer, it appears 20 K below the melting transition (T_m = 170 K). To facilitate comparison with experiment, quasielastic spectra calculated from the MD simulations were analyzed using the same models and fitting algorithms as for the neutron spectra. This combination of techniques gives a microscopic picture of the melting process in these two monolayers which is consistent with earlier neutron diffraction experiments. Butane melts abruptly to a liquid phase where the molecules in the *trans* conformation translationally diffuse while rotating about their center of mass. In the case of the hexane monolayer, the MD simulations show that the appearance of quasielastic scattering below T_m coincides with transformation of some molecules from *trans* to *gauche* conformations. Furthermore, if *gauche* molecules are prevented from forming in the simulation, the calculated incoherent scattering function contains no quasielastic component below T_m. Modeling of both the neutron and simulated hexane monolayer spectra below T_m favors a plastic phase in which there is nearly isotropic rotational diffusion of the *gauche* molecules about their center of mass, but no translational diffusion. The elastic scattering observed above T_m is consistent with the coexistence of solid monolayer clusters with a fluid phase, as predicted by the simulations. For $T/T_m \geq 1.3$, the elastic scattering vanishes from the neutron spectra where the simulation indicates the presence of a fluid phase alone. The qualitative similarities between the observed and simulated quasielastic spectra lend support to a previously proposed ''footprint reduction'' mechanism of melting in monolayers of flexible, rod-shaped molecules. © *1997 American Institute of Physics.* [S0021-9606(97)50237-6]

I. INTRODUCTION

Previous neutron diffraction experiments and molecular dynamics (MD) simulations have investigated the melting transition in monolayers of flexible rod-shaped molecules.[1] These studies compared the melting of monolayers composed of two different molecules in the *n*-alkane series [$CH_3(CH_2)_{n-2}CH_3$]: butane ($n=4$) and hexane ($n=6$) adsorbed on the graphite basal-plane surface. The MD simulations suggested a general mechanism of ''footprint reduction'' driving the melting transition. According to this mechanism, vacancies are introduced in the monolayer by motion of the adsorbate molecules normal to the graphite surface. These vacancies allow sufficient space on the surface for the molecules to disorder both translationally and rotationally. In the case of the shorter butane molecule, the footprint reduction is achieved by tilting of the molecules

away from the surface, whereas for the longer hexane molecule a conformational change occurs in which some molecules transform from the linear *trans* state to a more globular *gauche* state. It was proposed that this *trans–gauche* conformational change, occurring in some of the molecules below the melting point, initiated the melting process of the hexane monolayer.

Neutron diffraction experiments have found an orientationally ordered, two-sublattice monolayer structure for butane[2,3] and hexane[3,4] adsorbed on graphite at low temperature. For both monolayers, the rectangular unit cell is commensurate with the graphite (0001) surface[5] and contains two molecules with their long axis parallel to the surface and arranged in a herringbone pattern. In agreement with the MD simulations, the butane monolayer diffraction patterns indicated an abrupt melting transition with little short-range translational order above the melting point.[4,6,7] In the case of the hexane monolayer, the simulations predicted coexistence of the high-temperature liquid phase with small, solid monolayer clusters (characteristic dimension of ≤ 35 Å) having a

rectangular-centered (RC) structure.[1,8] The position and relative intensity of broad Bragg peaks present in the neutron diffraction patterns above the melting point[1,3,9] were consistent with the RC clusters revealed by the simulations. Thus, although the MD simulations predicted a melting point 25% higher than experiment for both the butane and hexane monolayers,[10] qualitative features of the diffraction patterns were consistent with the simulations.

Despite this agreement, some basic features of the footprint reduction mechanism suggested by the simulations could not be corroborated by the diffraction experiments that probe the static monolayer structure. In particular, they neither provided direct evidence of the tilting of the butane molecules nor the *trans–gauche* conformational change of hexane which were believed to initiate the monolayer melting process.

In order to learn more about the dynamics of the adsorbed molecules, particularly near the monolayer melting point, we have conducted a series of quasielastic neutron scattering experiments on butane and hexane monolayers adsorbed on graphite. In the case of the hexane monolayer, we planned to look for evidence in the quasielastic scattering below the melting point indicative of the *trans–gauche* conformational change found in the simulations. Similar measurements on the plastic phase of bulk butane in the temperature range from 110 to 135 K had found a broad quasielastic peak which was interpreted as resulting from conformational changes of the butane molecule.[11] We were also interested in comparing the amount of elastic scattering from these two monolayers at temperatures just above their melting point, looking for differences consistent with the presence of the solid RC clusters which the simulations had shown to coexist with the hexane monolayer liquid phase. In this way, quasielastic scattering could provide a further test of the melting mechanism which emerged from the MD simulations complementary to that provided by the neutron diffraction experiments.

An essential feature of our approach has been to generate the incoherent scattering function $S_{\text{inc}}(Q,\omega)$ of the monolayers from MD simulations and analyze it using the same models and computer codes used for the neutron spectra. We are not aware of this approach being applied previously to the study of diffusion in adsorbed monolayers. This detailed comparison of experiment and simulation leads to a description of the monolayer dynamics which is consistent with the footprint reduction mechanism of melting previously suggested for these monolayers.

II. TECHNIQUES

A. Experiment

The quasielastic neutron scattering experiments were performed on the QENS spectrometer at the Intense Pulsed Neutron Source of Argonne National Laboratory. As described elsewhere,[12] this spectrometer has an energy resolution width of about 70 μeV [full width at half maximum (FWHM)]. It has three separate analyzer-filter-detector as-

semblies which move together, allowing data to be collected at three different wave vector transfers **Q** simultaneously.

The chemical purity of the *n*-butane and *n*-hexane used as supplied[13] was 99.5% and 99%, respectively. These molecules were fully protonated in order to exploit the large incoherent neutron scattering cross section of hydrogen. It is estimated that the molecular carbon atoms contribute <3% of the total quasielastic intensity. For the substrate, we used a recompressed exfoliated graphite known as Papyex.[14] The sample consisted of a stack of disks, 1.0 cm in diameter and 10 cm high, having a mass of 12.9 g, placed in a cylindrical aluminum cell of wall thickness 0.050 cm. The substrate was prepared as in previous experiments,[15] and its surface area was calibrated by a nitrogen adsorption isotherm at 77 K.

For the butane experiment, background spectra from the graphite substrate were collected at room temperature using a single position of the QENS detector arms denoted as I, corresponding to wave vector transfers Q of 1.22, 1.61, and 2.53 Å^{-1}. However, for the hexane experiment, there was sufficient time to take background spectra at four settings of the QENS detector arms, yielding data at 12 Q's ranging from 0.57 to 2.53 Å^{-1}. The hexane background spectra were taken at a temperature of 13 K. In all cases, the background spectra were fit to a δ-function convoluted with the instrumental resolution function, and the integrated intensity, corrected for temperature effects,[16] was used as a measure of the graphite contribution to the elastic scattering.

All of the butane measurements were carried out at a single coverage of 0.88 layers, at which diffraction patterns had previously been obtained.[4,6,7] This coverage was sufficiently below monolayer completion that there was a negligible population of second-layer molecules at the highest temperatures investigated. At this coverage, the butane monolayer structure is partially commensurate with the graphite basal plane and contains two molecules arranged in a herringbone pattern.[2,3,5] The rectangular unit cell has dimensions $a = 8.52$ Å ($= 2\sqrt{3}a_g$ where a_g is the lattice constant of the graphite basal plane) and $b = 7.68$ Å. The majority of the *n*-butane monolayer data were collected at setting I of the QENS detector arms. Spectra were recorded at six temperatures in the range 13–149 K. At 140 K, a second setting of the detector arms was used to obtain spectra at Q's of 0.91, 1.87, and 2.40 Å^{-1}. These data were close enough in temperature to be combined with those taken at 138 K at position I to yield the Q dependence of the quasielastic scattering at a temperature about 22 K above the monolayer melting point.

The hexane experiments were performed at a submonolayer coverage of 0.95 layers where neutron,[3,4,9] x-ray,[3,9] and low-energy electron diffraction[17] experiments had shown the film to have a commensurate rectangular unit cell with lattice constants $a = 17.04$ Å ($= 4\sqrt{3}a_g$) and $b = 4.92$ Å ($= 2a_g$). Like the butane monolayer, the cell contains two molecules arranged in a herringbone pattern. Quasielastic spectra were taken at setting I of QENS at nine temperatures in the range 13 to 270 K. The Q dependence of the spectra was investigated at 13, 160, and 215 K by taking additional spectra at

seven Q's in the range 0.57–2.53 Å^{-1} at these temperatures.

B. Molecular dynamics simulations

The molecular dynamics (MD) simulation and the potentials used have been thoroughly described elsewhere,[1] so that a brief description will suffice here. The MD simulation employs a unified-atom model for each molecule in which the alkane methylene and methyl groups are replaced by pseudoatoms of mass 14 and 15 amu, respectively. The simulation was done within the NVT ensemble with bond lengths between neighboring pseudoatoms constrained to their equilibrium distances. All other molecular degrees of freedom have been included, totaling 9 for butane and 13 for hexane. The time step in the integration of the equations of motion was 0.002 ps in simulations up to temperatures of ∼150 K, 0.001 ps up to ∼250 K, and 0.0006 ps at higher temperatures. These time steps were found to give an acceptably small drift in the total energy over the duration of the simulation.

The simulation box size was chosen to be comparable to the coherence lengths found for the exfoliated graphite substrate used in the neutron diffraction and quasielastic scattering experiments.[6] For the butane system, the simulation box had dimensions of 63.01 Å×68.40 Å, with 128 molecules in the complete monolayer, while, for the hexane system, the box dimensions were 68.88 Å×68.17 Å, with 104 molecules in the complete monolayer.[18] The initial configurations for the simulations were the low-temperature herringbone ground states with all molecules in the *trans* configuration.[1]

One of the advantages of the MD approach is the capability of calculating dynamic properties, such as the incoherent scattering function $S_{inc}(Q,\omega)$, which can be readily compared to experimental results. In a typical low-temperature solid, $S_{inc}(Q,\omega)$ exhibits a sharp peak centered at energy transfer $\omega=0$, whose integrated intensity has a Debye–Waller dependence on Q. Any diffusive motion of the constituent molecules or atoms broadens this sharp peak.

The first step in the calculation of $S_{inc}(Q,\omega)$ is to generate the incoherent intermediate scattering function, which is a time-correlation function defined by

$$I_{inc}(\mathbf{Q},t) = \frac{1}{N}\sum_{i=1}^{N} \langle \exp[i\mathbf{Q}\cdot(\mathbf{r}_i(t+t_0)-\mathbf{r}_i(t_0))]\rangle, \quad (1)$$

where N is the number of atoms in the simulation and $\mathbf{r}_i(t)$ is the position vector of atom i at time t. The brackets $\langle\ \rangle$ denote a canonical average, here an average over initial times t_0. The data for calculation of $I_{inc}(\mathbf{Q},t)$ were generated by continuing calculations after an initial equilibration period of 150–200 ps. Since the neutron scattering experiments were performed on a polycrystalline substrate, the powder average of Eq. (1) was calculated as

$$\bar{I}_{inc}(Q,t) = \frac{1}{N}\sum_{i=1}^{N} \left\langle \frac{\sin[|\mathbf{Q}||\mathbf{r}_i(t+t_0)-\mathbf{r}_i(t_0)|]}{|\mathbf{Q}||\mathbf{r}_i(t+t_0)-\mathbf{r}_i(t_0)|}\right\rangle, \quad (2)$$

with $|\mathbf{r}_i(t+t_0)-\mathbf{r}_i(t_0)|$ computed by the method described by Allen and Tildesley.[19]

From the simulation, we can calculate the powder-averaged incoherent scattering function $S_{inc}(Q,\omega)$, defined as the Fourier transform of the incoherent intermediate scattering function

$$S_{inc}(Q,\omega) = \int_{-\infty}^{\infty} e^{i\omega t}\bar{I}_{inc}(Q,t)dt. \quad (3)$$

The energy or ω resolution of $S_{inc}(Q,\omega)$ is determined by the length of time over which the correlation function of Eq. (2) is calculated. The choice in these simulations was to reproduce the experimental resolution of 70 μeV. Accordingly, the incoherent intermediate scattering function has been determined up to 90 ps with a time interval of 0.75 ps.

$S_{inc}(Q,\omega)$ was calculated from Eqs. (2) and (3) for the butane and hexane simulations at a series of reduced temperatures T/T_m, covering the range of experimental temperatures. T_m is the monolayer melting point which, as noted previously, was 25% higher than the experimental value for both the butane and hexane monolayers.[10] $S_{inc}(Q,\omega)$ was fit to a sum of Gaussian and Lorentzian components, representing the elastic and quasielastic scattering, respectively. This parameterization was used to generate simulated spectra on an energy grid suitable for input to the same codes developed for analyzing the experimental spectra.

III. MODEL-INDEPENDENT DATA ANALYSIS

Our principal interest was to model the simulated and experimental quasielastic spectra to determine the nature of the diffusive motion in the butane and hexane monolayers near the melting transition. Before doing so, however, it was helpful to perform a simpler, model-independent analysis of the simulated and experimental spectra in order to assess how closely they agree, and to reveal any qualitative differences between the quasielastic scattering of the butane and hexane monolayers.

To accomplish this, we consider a scattering law similar to that used to parameterize the simulated spectra, namely, the sum of elastic and quasielastic components represented by a δ-function and a single Lorentzian, respectively,

$$S(Q,\omega) = A\,\delta(\omega) + \frac{B}{\pi}\left(\frac{\Gamma}{\Gamma^2+\omega^2}\right), \quad (4)$$

where Γ is the half width at half maximum of the Lorentzian. In the case of the simulated spectra, the δ-function component was replaced by a Gaussian. To fit the scattering law of Eq. (4) to the neutron quasielastic spectra, we must fold it with the QENS instrumental resolution function.[12] The quality of the fit so obtained is illustrated in Fig. 1 for the spectrum observed from 0.88 layers of butane adsorbed on Papyex at $Q=1.61$ Å^{-1} and a temperature of 149 K. The dotted and dashed curves are the δ-function and Lorentzian components of this best fit folded with the instrumental resolution function.

It is useful to begin the analysis by simply assessing the amount of elastic scattering in the spectra as a function of
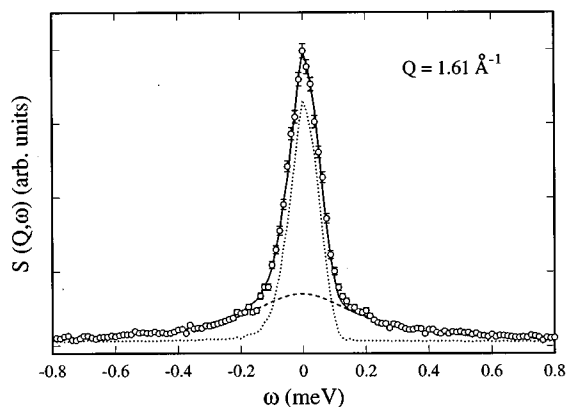
FIG. 1. Typical quasielastic spectrum from a butane monolayer at 149 K and a wave vector transfer $Q = 1.61$ Å^{-1}. The solid curve is the best fit to Eq. (4), the dotted curve is the δ-function component convoluted with the instrumental resolution function, and the dashed curve is the Lorentzian component convoluted with the resolution function. At this temperature the monolayer is a liquid, so all the butane scattering is contained in the Lorentzian component. The δ-function component is due solely to elastic scattering from the graphite substrate.

temperature. In Fig. 2, we have plotted for both the butane and hexane monolayers the temperature dependence of the ratio R of the integrated intensity of the δ-function component of the quasielastic scattering (after subtraction of the graphite substrate contribution) to the total integrated inten-

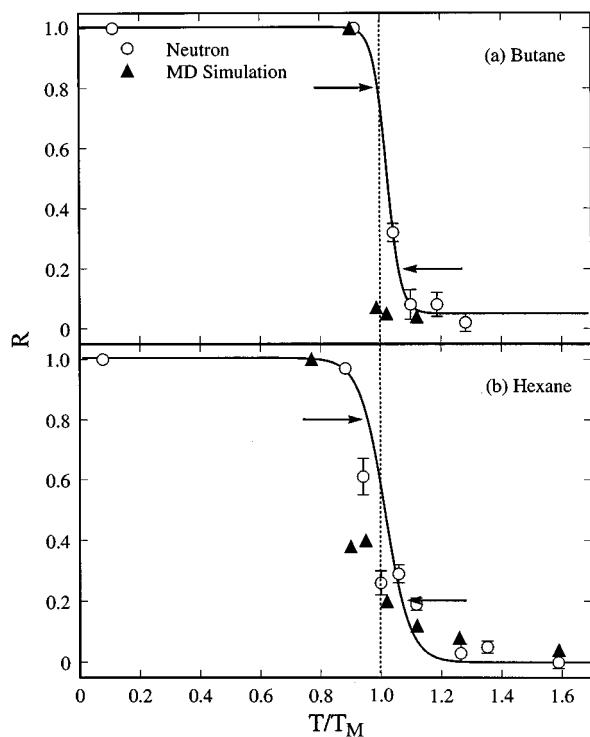FIG. 2. The intensity ratio R of the elastic to the total scattering for the monolayers at $Q = 1.61$ Å^{-1}: (a) butane and (b) hexane. The horizontal axis is the reduced temperature T/T_m, where T_m is the monolayer melting point. Open circles are the neutron scattering results, while the filled triangles were determined from the molecular dynamics simulations. The solid curves are fits of Eq. (5) to the neutron data.

sity. The reduced temperature T/T_m is used on the horizontal axis. From neutron and x-ray diffraction experiments, the melting point has been measured to be 116 for butane[6,7] and 170 K for hexane.[1,3,4,9]

The ratio R measures the fraction of the molecules exhibiting no diffusion on the time scale which the instrumental energy resolution allows us to sample i.e., which is characterized by a translational diffusion constant $\leqslant 0.2 \times 10^{-5}$ cm^2/s.[20] The constant value of $R = 1$ below T_m in Fig. 2(a) indicates the absence of diffusive motion below the butane monolayer melting point, whereas the decrease in R below the hexane monolayer melting point in Fig. 2(b) indicates an earlier onset of diffusion. This feature of the experimental data is reproduced by the quasielastic spectra generated from the MD simulation, as shown by the solid triangles in the plots.

To estimate the melting point and width of the transition from the measurement of R, we have fitted the neutron data in Fig. 2 to the form

$$R = C + \frac{D}{\exp\left[\dfrac{2 \ln 4(T - \tau_m)}{W}\right] + 1},\qquad(5)$$

which fits R well and is chosen for convenience. Here τ_m is the point of maximum slope and W measures the width of the transition region as the temperature interval in which R lies between values of 0.80 and 0.20 (see horizontal arrows in Fig. 2). The fits give $\tau_m = 118$ and 172 K for the butane and hexane monolayers, respectively, in good agreement with the melting points inferred from the diffraction experiments as noted above. The fit to Eq. (5) also shows the melting transition of the butane monolayer to be more abrupt ($W = 7.2$ K) than that of hexane ($W = 19$ K). It is interesting to note that, in the case of the hexane monolayer, the quasielastic spectra appear to give a larger width to the melting transition than the diffraction experiments. At the same coverage, the x-ray Bragg peak intensity falls from 90% of its low-temperature value to zero between 165 and 175 K, while the neutron diffraction pattern changes from one containing sharp peaks to a smaller number of broad peaks in the same temperature range.[3,9,21]

An explanation for this behavior is provided by the MD simulations, which show the presence of *gauche* molecules in the hexane monolayer below T_m and the coexistence of RC monolayer clusters with a fluid phase just above T_m. As noted in Sec. I, the RC phase has already been found to be consistent with broad-peak structure of the neutron diffraction patterns.[3,9] Thus, we associate the greater width of the melting transition inferred from the quasielastic spectra with both the formation of mobile *gauche* molecules below T_m and the coexistence of the fluid and RC phases above T_m. Further support for this interpretation is provided by detailed modeling of the quasielastic spectra described in the following sections.

Figure 3 shows the temperature dependence of the widths Γ of the Lorentzian component of Eq. (4) at $Q = 1.61$ Å^{-1}, as determined both from the quasielastic neu-
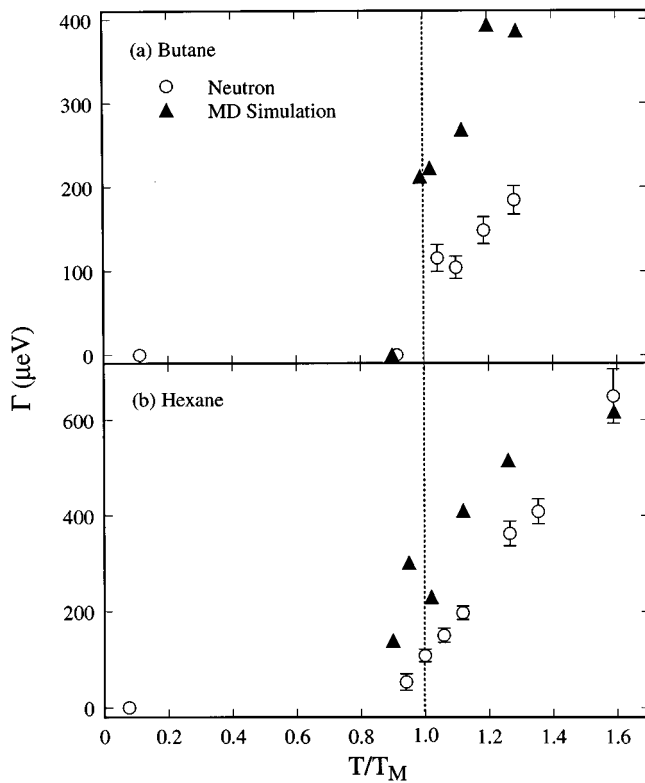
FIG. 3. Results of fitting Eq. (4) to the quasielastic spectra. The half width at half maximum of the Lorentzian component is plotted versus reduced temperature at $Q = 1.61$ Å^{-1}: (a) butane and (b) hexane. The open circles are the results from the neutron quasielastic spectra, while the filled triangles were determined from the MD simulations.

tron spectra and the spectra generated from the MD simulations. There is qualitative agreement between the experiment and the simulation in the following respects: (1) no broadening below the melting point is found for the butane monolayer, while it is present in the case of hexane; and (2) both monolayers show roughly the same rate of increase in the width of the quasielastic component as the temperature is raised above the melting point.

IV. QUASIELASTIC SCATTERING MODELS

A. Scattering functions

A more detailed picture of the diffusive motion in the butane and hexane monolayers can be obtained by applying some standard models used previously to describe molecular diffusion in physisorbed films.[22,23] We begin our discussion by considering the incoherent scattering functions for these models. The first of these represents a simple model of translational diffusion in which the molecular center of mass executes random Brownian motion. This model has been used previously in the analysis of quasielastic neutron scattering from ethane monolayers adsorbed on graphite,[22,23] and yields the following incoherent scattering function:

$$S_B(Q_\parallel, \omega) = \frac{1}{\pi} \frac{D_t Q_\parallel^2}{\omega^2 + (D_t Q_\parallel^2)^2}, \tag{6}$$

where $Q_\parallel$ is the component of $\mathbf{Q}$ parallel to the graphite surface, and D_t is the translational diffusion constant.

We have considered two different models of rotational diffusion. In the first of these, the molecule rotates about a single axis. For example, bulk butane has a high-temperature plastic phase in which the molecules are translationally ordered but rotate about their long axis.[24] Such a phase is apparently not observed for the butane monolayer, which showed no quasielastic scattering below T_m. On the other hand, evidence of uniaxial rotation has been found below the melting point of two different monolayer phases of the shortest alkane, ethane [CH_3CH_3], adsorbed on graphite. Quasielastic neutron spectra were consistent with the molecule rotating about the C–C bond in both the herringbone S_1 phase (bond parallel to the surface) as well as the higher-density hexagonal S_3 phase (bond perpendicular to the surface).[23]

We have considered models of uniaxial rotation for the hexane monolayer in which the molecules rotate either about their long axis (the axis with the lowest moment of inertia) oriented parallel to the surface, or about an axis normal to the surface through the molecular center of mass. The incoherent scattering function for such uniaxial rotation is given by[25]

$$S_{\mathrm{uni}}(Q_\perp, \omega) = \sum_{i=1}^{N} \left[J_0^2(Q_\perp r_i) \delta(\omega) \right.$$
$$\left. + \frac{2}{\pi} \sum_{m=1}^{\infty} J_m^2(Q_\perp r_i) \frac{m^2 D_r}{\omega^2 + (m^2 D_r)^2} \right], \tag{7}$$

where $Q_\perp$ is the component of $\mathbf{Q}$ in a plane perpendicular to the rotation axis, the J_m are mth-order Bessel functions of the first kind, r_i is the distance of the ith atom from the axis of rotation and N is the number of atoms in the molecule. Five terms of the sum over m in Eq. (7) were retained as higher-order terms made insignificant contributions over the Q range of the experiment.

The other model of rotational diffusion which we considered was one in which the molecules rotated isotropically about their center of mass. This model had been applied successfully to diffusion in the ethane monolayer phases on graphite at higher temperatures.[22,23] The incoherent scattering function for this model is given by[25,26]

$$S_{\mathrm{iso}}(Q, \omega) = \sum_{i=1}^{N} \left[j_0^2(Q r_i) \delta(\omega) + \frac{1}{\pi} \sum_{m=1}^{\infty} (2m+1) \right.$$
$$\left. \times j_m^2(Q r_i) \frac{m(m+1)D_r}{\omega^2 + [m(m+1)D_r]^2} \right], \tag{8}$$

where the j_m are mth-order spherical Bessel functions and r_i is the distance of the ith atom from the center of mass of the molecule. The sum over m was terminated at the sixth term, as higher-order contributions were negligible over the Q range of the experiment. In this model, the ith atom moves on the surface of a sphere of radius r_i whose center is at the molecular center of mass. For comparison with the neutron quasielastic spectra, only the H-atom radii are included, while in the case of the simulated spectra, the radii are taken as the distance of the pseudoatoms from the molecular center

of mass. The butane molecule was assumed to be in the *trans* conformation. Two different conformations of the hexane molecule were considered: one in which the molecules were *trans* and the other in which they had a single, terminal *gauche* defect. Conformations with more than one *gauche* defect were ignored, both for the sake of simplicity and because the MD simulations had indicated them to be less probable below the hexane monolayer melting point.

We analyzed the quasielastic scattering of the butane and hexane monolayers above their melting point, assuming a combination of rotational and translational diffusion. To simplify the analysis, the translational and rotational motions of the molecules were assumed to be independent. In this approximation, the intermediate scattering function Eq. (1) is a product of a center-of-mass translational term and one representing rotation about the molecular center of mass. The corresponding incoherent scattering function can then be written as a convolution of translational and rotational terms:[25,27]

$$S_{\text{tot}}(Q,\omega) = S_{\text{iso}}(Q,\omega) \otimes S_B(Q_{\parallel},\omega). \tag{9}$$

As was the case below the monolayer melting point, both a *trans* conformation and one with a single, terminal *gauche* defect were considered for the hexane molecules. However, only the *trans* conformation of butane was used, since the MD simulations had shown *gauche* conformers to be absent in the monolayer at temperatures near the melting point.

B. Implementation

Due to the dependence of the incoherent scattering functions in Eqs. (6), (7), and (9) on either $Q_{\parallel}$ or $Q_{\perp}$, it is necessary to average the scattering functions over the orientational distribution of graphite crystallites in our polycrystalline substrate before comparing with the neutron quasielastic spectra. We let $\rho(\gamma)$ be the orientational distribution function, where γ is the angle between the normal to the scattering plane and a crystallite surface normal so that $\tan \gamma = Q_{\perp}/Q_{\parallel}$. The appropriately averaged scattering law, which we have applied to both the butane and hexane monolayers above their respective melting points, is then

$$S^{\text{avg}}(Q,\omega) = \int_0^{\pi} \rho(\gamma) S(Q,\omega) \sin \gamma \, d\gamma, \tag{10}$$

where $S(Q,\omega)$ is one of the incoherent scattering functions defined by Eqs. (6)–(9). Note that to compare Eq. (10) with $S_{\text{inc}}(Q,\omega)$ calculated from the simulation, one sets $\rho(\gamma)$ equal to a constant, since $S_{\text{inc}}(Q,\omega)$ is calculated as an isotropic average.

The integration over the orientational distribution in Eq. (10) was implemented numerically as part of our fitting algorithm. As in previous studies,[28] we used a two-component distribution with 70% of the graphite crystallites oriented isotropically and 30% having a Gaussian distribution about the scattering plane. A full width at half maximum of 30° for the Gaussian component was assumed as before.[28] We also considered the effect of altering the crystallite angular distribution $\rho(\gamma)$ on the analysis of the neutron spectra. A purely isotropic distribution resulted in translational diffusion con-

TABLE I. Parameters derived from fitting the *neutron* quasielastic spectra of the butane and hexane monolayers to a model of translational/isotropic rotational diffusion represented by Eq. (9). The analysis used the all-*trans* geometry of butane while the hexane analysis was performed with a molecule having a single terminal *gauche* defect as discussed in the text. When the population of localized molecules vanishes ($f_m=1$), $\langle u^2 \rangle$ has no significance.

T (K)	T/T_m	f_m	$\langle u^2 \rangle$ (Å^2)	D_t (10^{-5} cm^2/s)	D_r (10^9/s)
			Butane		
106	0.91	0	0.06±0.03	0[a]	0
121	1.04	0.7	0.06±0.03	1.00±0.05	1.3±0.4
128	1.10	1.0	⋯	1.22±0.06	0.8±0.1
139	1.20	1.0	⋯	1.77±0.12	2.6±0.5
149	1.28	1.0	⋯	1.7±0.4	7.9±2.6
			Hexane		
150	0.88	0.17	0.06±0.03	0[a]	6.6±0.7
160	0.94	0.31	0.06±0.02	0[a]	10±0.7
170	1.00	0.59	0.09±0.03	0	15±0.6
180	1.06	0.78	0.16±0.05	0	16±0.6
190	1.12	0.92	0.15±0.05	0.14±0.07	19±1.3
215	1.26	1.00	⋯	1.7±0.5	45±6
230	1.35	1.00	⋯	2.1±0.4	28±6
270	1.59	1.00	⋯	3.5±0.7	59±7

[a]No translational diffusion assumed.

stants D_t about two times greater than those deduced using the two-component distribution. We interpret these larger values as providing an upper bound to D_t. As expected, assuming a purely isotropic distribution made no significant change in the diffusion constants inferred for isotropic rotation about the molecular center of mass. The diffusion constants listed in Table I and plotted in Fig. 6 were determined assuming the two-component distribution.

The computer code used to analyze both the neutron and simulated data was constrained to fit simultaneously the quasielastic spectra at all of the Q's investigated at each temperature. The fit could be made to any one of the scattering functions given by Eqs. (6)–(9) averaged over the crystallite orientation distribution as in Eq. (10). In fitting the neutron spectra, the total δ-function intensity was allowed to vary independently for each spectrum. The scattering from the graphite substrate was modeled as an additive contribution to the δ-function component, with its magnitude determined from the measured graphite background corrected by the Debye–Waller factor appropriate to each temperature.[16]

At the lowest temperatures, the adsorbed molecules contribute only to the δ-function component of the spectra. However, upon heating, we found a range of temperatures near the melting point over which only a fraction f_m of the molecules diffuse where f_m is calculated from the intensity ratio of the quasielastically broadened component to the total scattering. This fraction is listed in Tables I and II as a function of temperature for both the neutron and simulated quasielastic spectra. The residual elastic intensity from the localized molecules follows a Debye–Waller ($e^{-Q^2 \langle u^2 \rangle}$) dependence on Q, where the corresponding $\langle u^2 \rangle$ is given in Tables I and II. Thus near the melting point of the monolayers, we can think of the adsorbed monolayer as comprising two populations: localized molecules from which there is only elastic scattering, and mobile molecules which contrib-

TABLE II. Parameters derived from fitting the *simulated* quasielastic spectra of the butane and hexane monolayers to a model of translational/isotropic rotational diffusion represented by Eq. (9) as presented in Table I.

T (K)	T/T_m	f_m	$\langle u^2 \rangle$ (Å^2)	D_t (10^{-5}cm^2/s)	D_r (10^9/s)
			Butane		
137	0.90	0	⋯	0^a	0
150	0.99	1.0	⋯	2.4	25
155	1.02	1.0	⋯	2.7	28
170	1.12	1.0	⋯	3.4	36
182	1.20	1.0	⋯	3.0	39
196	1.29	1.0	⋯	4.4	38
			Hexane		
170	0.77	0	0.17	0^a	0
200	0.90	0.69	0.17	0^a	11
210	0.95	0.68	0.24	0^a	26
225	1.02	0.82	0.45	0.3	32
249	1.12	1.00	⋯	2.1	43
280	1.26	1.00	⋯	4.2	39
353	1.59	1.00	⋯	9.3	52

^{a}No translational diffusion assumed.

ute the quasielastic component to the spectra. The scattering law appropriate to such a two-component system is then given by

$$S_{tot}^{avg}(Q,\omega) = (1-f_m)\delta(\omega)e^{-Q^2\langle u^2\rangle} + f_m S^{avg}(Q,\omega), \quad (11)$$

where $S^{avg}(Q,\omega)$ is defined in Eq. (10).

V. RESULTS

We now examine the results of applying the diffusion models described in the previous two sections. For both monolayers, we divide the discussion into two temperature regimes corresponding to below and above the monolayer melting point, respectively.

A. Below melting

Since the butane monolayer showed no quasielastic scattering below its melting point, we begin by considering the quasielastic spectra of the hexane monolayer below its observed melting point $T_m = 170$ K. Above a reduced temperature $T/T_m = 0.88$, the quasielastic scattering in the neutron spectra is intense enough to be able to distinguish clearly between the rotational models discussed in the previous section. We compared the fits to observed and simulated spectra of the hexane monolayer below its melting point for the two different models of rotational diffusion in the absence of translational diffusion. The isotropic rotation model yielded the best fit to both the neutron and simulated quasielastic spectra above $T/T_m = 0.88$. As can be seen in Fig. 4 for the neutron spectrum at $Q = 1.01$ Å^{-1} at $T/T_m = 0.94$, the model of uniaxial rotation predicts too small of a quasielastic component. At other Q values, fitting the neutron spectra with the uniaxial rotation model resulted in unphysical parameters, such as a negative intensity, given to the elastic component. Similar behavior was found when the uniaxial model was applied to the simulated spectra.

While fits to the neutron and simulated quasielastic spectra could distinguish between models of uniaxial and isotro-
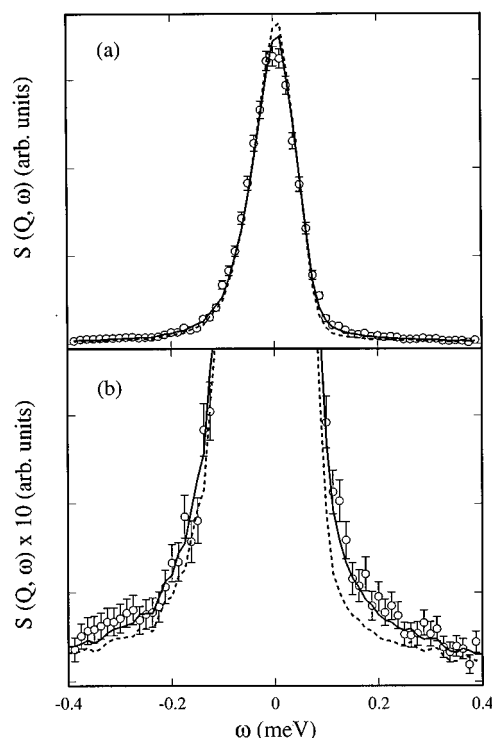

FIG. 4. (a) Neutron quasielastic spectra of the hexane monolayer at a temperature of 160 K ($T/T_m = 0.94$) at $Q = 1.01$ Å^{-1}. (b) Same as in (a) except magnified ten times. Solid lines are fits to the model of isotropic rotation, while the dashed lines are fits to the uniaxial rotation model. The elastic contribution from the graphite substrate has been subtracted from both the data and the fit. Note that the asymmetry in the line shapes results from the instrumental resolution function.

pic rotational motion for the hexane monolayer below its melting point, they were insensitive to the molecular conformation. Both the *trans* conformation and one having a single terminal *gauche* defect yielded the same values of the mobile fraction f_m and rotational diffusion constant D_r within the uncertainties listed in Table I. We will see in the next section that there is compelling evidence from the simulation that it is the *gauche* hexane molecules which are responsible for the quasielastic component in the spectra below the melting point. Thus to facilitate comparison between analysis of the experimental and simulated spectra, all fitting parameters reported in Tables I and II and in the following figures were determined assuming a single terminal *gauche* defect in the hexane molecule.

While fits of the isotropic rotation model to the neutron and simulated spectra below the hexane monolayer melting point reveal the same qualitative features, we consistently find the experimental spectra to give smaller values of mobile fraction f_m and the mean-squared displacement $\langle u^2 \rangle$ of the localized fraction of molecules. In addition, the rotational diffusion constants D_r of the mobile population are two to three times smaller in the experimental fits. These results are consistent with the larger widths Γ found for the simulated spectra in the single-Lorentzian plus δ-function analysis in Sec. III. Reasons for these quantitative differences will be discussed in the next section.
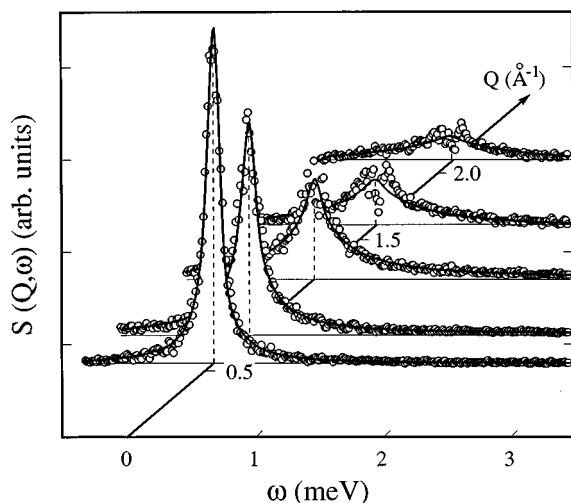
FIG. 5. Neutron quasielastic spectra of the hexane monolayer at a temperature of 215 K ($T/T_m = 1.26$). Solid lines are the best fits to the data of the random translational/isotropic rotational diffusion model described by Eq. (9). The elastic contribution from the graphite substrate has been subtracted from both the data and the fit.
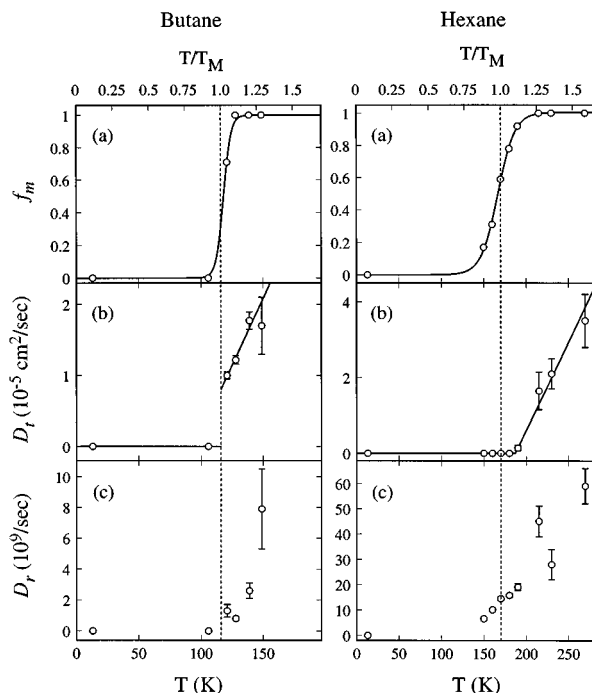

FIG. 6. Results of fitting the neutron quasielastic spectra with the model of random translational diffusion/isotropic rotational diffusion represented by Eq. (9). Temperature dependence of the fitting parameters: (a) the fraction f_m of mobile molecules; (b) the translational diffusion constant D_t; and (c) the rotational diffusion constant D_r. The left column contains the butane monolayer results, while the right column shows the results from the hexane monolayer. Solid curves are fits to the data as discussed in the text.

B. Above melting

For temperatures greater than the melting point, both the hexane and butane spectra were modeled assuming a combination of isotropic rotational and random translational diffusion described by using the incoherent scattering function of Eq. (9) in Eq. (11). The representative neutron spectra in Fig. 5 of the adsorbed hexane monolayer at 215 K illustrate the quality of the fits obtained with this model after folding with the instrumental resolution function. At this temperature, no residual elastic intensity is observed, so that all of the hexane molecules participate in the diffusive motion ($f_m = 1$). Note, that unlike Fig. 1, the elastic contribution from the Papyex substrate has been subtracted in order to enhance sensitivity to the quasielastic scattering.

As was the case below the melting point, fits to the experimental spectra generally give rotational diffusion constants D_r about two times smaller than for the simulation, consistent with the larger widths Γ found for the simulated spectra in the Lorentzian plus δ-function analysis. The same is true for the translational motion, which begins above the melting point with the diffusion constants D_t inferred from the neutron spectra being about a factor of two to three smaller than for the simulation. An even larger effect is seen for the butane monolayer above its melting point, where the experimental values are smaller than for the simulation by more than an order of magnitude for D_r and a factor of two to three in the case of D_t.

The temperature dependence of the parameters obtained from fitting the neutron quasielastic spectra of the butane and hexane monolayers is presented in Fig. 6, where f_m, D_t, and D_r are plotted versus temperature. The solid curve in Fig. 6(a) is a fit to the f_m data with a function similar to that in Eq. (5). These fits give $\tau_m = 118$ and 167 K as the temperature of maximum slope for the butane and hexane monolayers, respectively, in reasonable agreement with the values

obtained in the δ-function plus Lorentzian analysis. Once the molecules begin to diffuse, D_t increases linearly with temperature at a rate of 0.04×10^{-5} and 0.05×10^{-5} cm²/s/K for butane and hexane, respectively [see Fig. 6(b)]. We also see that the rotational diffusion constant increases rapidly with temperature above T_m for butane, while for hexane a significant increase in the rotational mobility of some molecules begins below T_m [see Fig. 6(c)].

For comparison, Fig. 7 presents the temperature dependence of the same parameters as in Fig. 6, but now derived from fitting the *simulated* quasielastic spectra to the model of combined translational and isotropic rotational diffusion. Despite the larger values of the translational diffusion constant D_t at each temperature, we again find a roughly linear increase with temperature, giving slopes of 0.04×10^{-5} and 0.07×10^{-5} cm²/s/K for butane and hexane, respectively [see Fig. 7(b)]. These slopes are comparable to those obtained from analyzing the neutron spectra. D_r exhibits the same qualitative temperature dependence as was seen in Fig. 6 for the neutron spectra, increasing significantly below T_m for the hexane monolayer and increasing rapidly for both monolayers above T_m [see Fig. 7(c)].

VI. DISCUSSION

As in the previous section, we organize our discussion by considering the quasielastic spectra of each monolayer, first below its melting point, and then above. In the case of
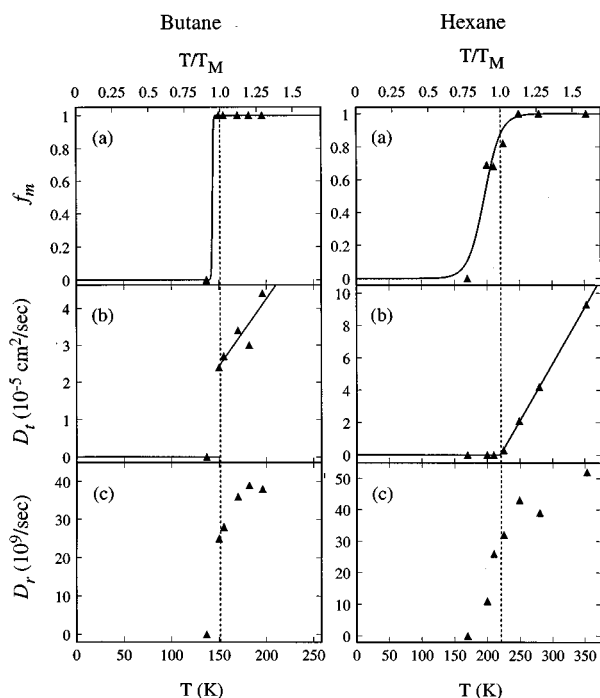
FIG. 7. Results of fitting the simulated quasielastic spectra with the model of random translational diffusion/isotropic rotational diffusion represented by Eq. (9). The temperature dependence of the fitting parameters f_m, D_t, and D_r is presented as in Fig. 6.

the hexane monolayer, we use the results of the MD simulation to give a more detailed interpretation of the quasielastic spectra than is possible from modeling the neutron scattering data alone.

A. Below melting

Neither the neutron nor the simulated spectra of the butane monolayer exhibited quasielastic broadening below melting. These results are consistent with the abrupt, first order melting transition observed at monolayer coverage in both neutron diffraction[4,6,7] and specific heat experiments.[29]

Turning to the hexane monolayer, the analysis of the neutron quasielastic spectra below T_m is in qualitative agreement with the simulation, but differs in quantitative details. Generally, the amount of molecular motion inferred from the experiment is less than that predicted by the simulation. This is reflected in the smaller values of mobile fraction f_m, $\langle u^2 \rangle$, and D_r below the monolayer melting point (see Tables I and II). The differences in D_r between simulation and experiment cannot be attributed to the use of pseudoatoms in the molecules of the simulation. Although pseudoatoms result in a smaller moment of inertia about the long axis of the molecule, they reproduce rather well the moments of inertia about the other two principal axes of rotation, the ones relevant to the model of isotropic rotation, as discussed below.

We believe the principal reason for the greater degree of molecular motion exhibited in the simulation than the experiment is the higher absolute temperature of the melting point in the simulation. The simulation gives a melting point of the butane monolayer of 152 compared to the value of 116 K

obtained by neutron diffraction,[6,7] while for hexane the melting points are at 170 (neutron) and 221 K (simulation).[3,4] The effect of the higher melting point of both monolayers in the simulations could be checked by using an alternative molecule–substrate interaction which results in melting temperatures closer to those observed.[10] As will be discussed below, further work is needed to elucidate other possible causes of this discrepancy between experiment and simulation.

Fits of both the neutron and simulated quasielastic spectra favor a model of isotropic rotation about the molecular center of mass rather than rotation about a single molecular axis below the hexane monolayer melting point. In all cases, uniaxial rotation produced too large of an elastic component in the spectra. The reason for this can be seen by comparing the incoherent scattering functions in Eqs. (7) and (8). We see that for uniaxial rotation, S_{uni} depends on $Q_\perp$, the component of Q in a plane perpendicular to the axis of rotation, whereas, for isotropic rotation, S_{iso} depends only on Q. Since $Q_\perp \lesssim Q$ and J_0 is a decreasing function for small arguments, whereas the J_m ($m > 0$) are increasing in the same range, the elastic component of the scattering will be enhanced in the case of uniaxial rotation when the polycrystalline average in Eq. (10) is performed.

We should emphasize, however, that the isotropic and uniaxial rotational models may represent only two extreme types of motion. The actual motion may be somewhere in between. We interpret our results as indicating that the rotational motion is closer to isotropic than uniaxial. One possible explanation for this is that it is mostly *gauche* molecules which are rotating. They are more globular in shape and, therefore, a single rotational axis is not selected energetically. Unfortunately, we could not verify this interpretation from analysis of the neutron and simulated quasielastic spectra, since fits to the spectra were insensitive to the molecular conformation. In particular, we did not observe a feature in the quasielastic spectra due to the *trans–gauche* conformational change as was interpreted for bulk butane.[11]

To address the question of the conformation of the diffusing molecules, we must rely on the MD simulations as justified by their strong qualitative agreement with the quasielastic experiments. Our earlier simulations[1] had shown that about 10% of the molecules were in the *gauche* conformation at a reduced temperature $T/T_m = 0.95$. When the *trans*-to-*gauche* conformational change was suppressed in the simulation so that no *gauche* molecules formed at temperatures below T_m, the melting point of the hexane monolayer increased. We have extended this analysis here by calculating the quasielastic spectra for monolayers without *gauche* molecules and find no broadening at $T/T_m = 0.95$. Thus, we conclude from the simulations that the presence of quasielastic broadening at that temperature coincides with the appearance of *gauche* molecules.

However, the question remains as to whether it is only the *gauche* molecules which are diffusing or whether their presence also facilitates diffusion of some of the *trans* molecules below the melting point. In this regard, we note that the value $f_m = 0.68$ obtained for the mobile fraction of mol-

ecules at $T/T_m = 0.95$ (see Table II) by fitting the simulated quasielastic spectra with S_{iso} substituted into Eq. (11), is considerably larger than the 10% fraction of *gauche* molecules obtained by analyzing the dihedral-angle distribution[1] at this temperature. This discrepancy may result from not all of the mobile molecules having a single terminal *gauche* defect as we have assumed in fitting the quasielastic spectra. The presence of a small number of *gauche* molecules could create space on the graphite surface which would facilitate rotation of *trans* molecules. This possibility is difficult to test due to the large number of parameters in a model in which the rotationally diffusing molecules can have more than one conformation.

B. Above melting

The MD simulations are also quite helpful in interpreting the different behavior observed in the neutron quasielastic spectra of the butane and hexane monolayers above their respective melting points. According to the simulation, the butane monolayer melts abruptly to a liquid phase in which *all* of the molecules rotate about their center of mass while undergoing translational diffusion. In contrast, the hexane monolayer does not attain a mobile fraction $f_m = 1$ until 27 K above T_m. We associate the elastic component in the simulated quasielastic spectra in the temperature range $1.0 < T/T_m < 1.1$, with the solid RC clusters found to coexist with a fluid phase in the earlier simulations, and whose presence explained the broad peaks observed in the neutron diffraction patterns.[1,3,9] At higher temperatures, the simulations indicated that the RC clusters themselves melt rather than diffuse through the coexisting fluid phase.[1] This behavior is consistent with the increase in the mean-squared displacement $\langle u^2 \rangle$ of the localized molecules to 0.45 Å^2 at $T/T_m = 1.02$ as inferred from the simulated spectra (see Table II).

Comparing fits of the neutron and simulated spectra of both the hexane and butane monolayers to Eq. (9) above their respective melting points, we again find qualitative similarities but some quantitative differences. In all cases, a model of isotropic diffusion about the molecular center of mass remains favored over one of uniaxial rotation. The neutron spectra still yield smaller values of D_t and D_r just above the melting point of both monolayers. Larger values of D_t can be obtained from the neutron spectra if an isotropic crystallite distribution is assumed for the graphite substrate, but this is unlikely to explain the discrepancy in D_t completely because of the larger widths Γ found for the simulated spectra in the model-independent analysis in Sec. III (see Fig. 3).

These results, again, point to the simulation overestimating the degree of motion in the monolayer near the melting point. We note, though, that for the hexane monolayer at the highest temperatures ($T/T_m \geq 1.26$), the discrepancy between the values of D_r and Γ derived from the neutron spectra and those derived from the simulated spectra diminishes.

It is interesting to compare the magnitude of the translational diffusion constants extracted from the monolayer neutron spectra with those of the corresponding bulk liquids. At 150 K, D_t of bulk butane is measured to be 0.65

$\times 10^{-5}$ cm^2/s,[30] considerably less than our measured monolayer value of $1.7 \pm 0.4 \times 10^{-5}$ cm^2/s. Similarly, for bulk hexane $D_t = 1.3 \times 10^{-5}$ cm^2/s at 214 K (Ref. 30) compared to the monolayer value of $1.7 \pm 0.5 \times 10^{-5}$ cm^2/s. This behavior is like that observed previously for ethane adsorbed on graphite, where the monolayer D_t at 122 K was approximately three times larger than its bulk value at the same temperature.[23] More recently, D_t has been measured by He-beam scattering for an octane monolayer adsorbed on Cu (111).[31] The reported value exceeded the upper bound for the bulk D_t by a factor of approximately six.

Thus we see a general trend of larger values of D_t for monolayers of short *n*-alkanes adsorbed on a solid substrate than found in the bulk liquids. Rather than speculate on the reason for this, we prefer simply to emphasize the need for more simulation work both on bulk and monolayer phases of the alkanes to address this question.

Similar comparisons are more difficult to make for the rotational diffusion constant. A neutron quasielastic study of bulk liquid butane at 190 K reports a D_r of 277×10^9/s.[24] Our measurements on monolayer butane extend only to 149 K, but a reasonable extrapolation to 190 K [using an Arrhenius fit to the data in Fig. 6(c)] results in a value of 125×10^9/s, considerably less than the bulk value. Also, we note that the values of D_r, which we have inferred, are in the same range as those previously determined for the liquid monolayer phase of ethane adsorbed on graphite.[22]

VII. CONCLUSION

To summarize, we find at least qualitative agreement between the neutron and simulated quasielastic spectra near the melting points of both the butane and hexane monolayers using the model-independent analysis in Sec. III. In both the neutron and simulated spectra, only an elastic component is present for butane monolayer below its melting point. Both the neutron experiment and the simulation show an abrupt onset of the quasielastic component for the butane monolayer at its melting point and a concomitant disappearance of the elastic scattering. In the case of the hexane monolayer, a quasielastic component to the spectra appears below its melting point at a reduced temperature $T/T_m \sim 0.9$, while an elastic component persists up to $T/T_m \sim 1.3$. The width of the quasielastic component increases roughly linearly with temperature for both monolayers.

Based on our MD simulation, we have developed the following microscopic models for the diffusive motion in the butane and hexane monolayers. The butane monolayer melts abruptly to a liquid phase in which molecules in their *trans* state rotate about their center of mass while diffusing translationally.

In contrast, melting of the hexane monolayer is preceded ($T/T_m \sim 0.9$) by the formation of a small fraction of mobile molecules which may be predominantly in a *gauche* state and which diffuse rotationally about a *fixed* center of mass. At the monolayer melting point, hexane molecules in the mobile fraction begin to diffuse translationally as well as rotationally. The mobile fraction increases in size above the

melting point, reaching unity at $T/T_m \sim 1.3$. In this temperature range, the MD simulation predicts the coexistence of small, RC clusters which coexist with the fluid phase represented by the mobile fraction. The presence of these RC clusters is consistent with observed neutron diffraction patterns. At higher temperatures, the hexane monolayer exists in a fluid phase of predominantly *gauche* molecules in which, as in the case of the butane monolayer, molecules translationally diffuse while rotating about their center of mass.

The quasielastic scattering results and MD simulations presented here complement previous neutron diffraction experiments and simulations of melting in these alkane monolayers. By correlating the quasielastic scattering, which appears below the melting point of the hexane monolayer, with the appearance of *gauche* molecules, they support the ''footprint reduction'' melting mechanism proposed earlier. The quasielastic scattering also provides direct evidence above the hexane monolayer melting point of a fluid phase coexisting with the solid monolayer clusters whose presence had been inferred from the previous diffraction experiments and simulations.

While supporting the ''footprint reduction'' melting mechanism, the quasielastic neutron scattering experiments and simulations presented here have also raised some questions about diffusion in these monolayers which future work might address. These include: (1) Is the rotational motion of the diffusing molecules strictly isotropic or is it more complex for these nonspherical molecules? (2) While rotational diffusion below the melting point of the hexane monolayer is associated with the appearance of *gauche* molecules, are some *trans* molecules also rotationally diffusing? (3) Why do the simulations tend to give a greater degree of molecular motion than the experiment near the melting point? and (4) Why do the monolayer translational diffusion constants tend to be larger than in bulk? Neutron experiments with greater energy resolution and much larger scattered intensities, as well as longer simulations without the pseudoatom approximation, may yield more definitive answers to these questions.

ACKNOWLEDGMENTS

[1] F. Y. Hansen and H. Taub, Phys. Rev. Lett. **69**, 652 (1992); F. Y. Hansen, J. C. Newton, and H. Taub, J. Chem. Phys. **98**, 4128 (1993); F. Y. Hansen and H. Taub, in *Phase Transitions in Surface Films 2*, Vol. 267 of *NATO Advanced Study Institute, Series B: Physics*, edited by H. Taub, G. Torzo, H. J. Lauter, and S. C. Fain, Jr. (Plenum, New York, 1991), p. 153.

[2] K. W. Herwig, J. C. Newton, and H. Taub, Phys. Rev. B **50**, 15287 (1994).

[3] J. C. Newton, Ph.D. thesis, University of Missouri–Columbia, 1989.

[4] H. Taub, in *The Time Domain in Surface and Structural Dynamics*, Vol. 228 of *NATO Advanced Study Institute, Series C: Mathematical and Physical Sciences*, edited by G. J. Long and F. Grandjean (Kluwer, Dordrecht, 1988), p. 467.

[5] The butane monolayer is only partially commensurate with the graphite (0001) surface but becomes completely commensurate at higher coverage (see Ref. 2).

[6] G. J. Trott, Ph.D. thesis, University of Missouri–Columbia, 1981.

[7] G. J. Trott, H. Taub, F. Y. Hansen, and H. R. Danner, Chem. Phys. Lett. **78**, 504 (1981).

[8] The RC phase has been corroborated in subsequent simulations by G. H. Peters and D. J. Tildesley, Langmuir **12**, 1557 (1996).

[9] J. C. Newton, J. R. Dennison, S.-K. Wang, H. Taub, and F. Y. Hansen (unpublished).

[10] Better agreement has been obtained in subsequent MD simulations by selecting an alternative molecule–substrate interaction potential. See, E. Velasco and G. H. Peters, J. Chem. Phys. **102**, 1098 (1995).

[11] K. F. Bradley, S.-H. Chen, and T. O. Brun, J. Chem. Phys. **95**, 5273 (1991).

[12] K. F. Bradley, S.-H. Chen, T. O. Brun, R. Kleb, W. A. Loomis, and J. M. Newsam, Nucl. Instrum. Methods A **270**, 78 (1988).

[13] Matheson, Inc. and Fisher Scientific supplied the butane and hexane, respectively.

[14] Manufactured by Le Carbone Lorraine, Departément Produits Spéciaux, 37 à 41 rue Jean Jaures, 92231 Gennevilliers, France.

[15] S.-K. Wang, J. C. Newton, R. Wang, H. Taub, J. R. Dennison, and H. Shechter, Phys. Rev. B **39**, 10331 (1989).

[16] The intensity of the graphite elastic scattering was assumed to have a temperature dependence described by a Debye–Waller factor $[I(T) = I(0)\exp -Q^2 \langle u^{2(T)} \rangle]$ with $u^2(T)$ determined from the temperature dependence of the (002) Bragg peak of a different Papyex sample.

[17] J. Krim, J. Suzanne, H. Shechter, R. Wang, and H. Taub, Surf. Sci. **162**, 446 (1985).

[18] The number of molecules in the simulation box represented a complete monolayer for the potential energy parameters selected in the simulation. This number was determined on the basis of a calculated zero-temperature monolayer structure (see Ref. 1).

[19] M. P. Allen and D. J. Tildesley, *Computer Simulation of Liquids* (Clarendon, Oxford, 1987).

[20] The QENS spectrometer is sensitive to a change in linewidth on the order of $\Delta\Gamma = 15$ μeV in Eq. (4). At a wave vector transfer $Q = 1$ Å^{-1}, this corresponds to a translational diffusion constant of 0.2×10^{-5} cm^2/s.

[21] As discussed in Ref. 3, the x-ray and neutron structure factors for the RC phase differ.

[22] J. P. Coulomb, M. Bienfait, and P. Thorel, Faraday Discuss. Chem. Soc. **80**, 79 (1985).

[23] J. P. Coulomb and M. Bienfait, J. Phys. Paris **47**, 89 (1986).

[24] K. Refson and G. S. Pawley, Acta Crystallogr. B **42**, 402 (1986).

[25] M. Bée, *Quasielastic Neutron Scattering* (Adam Hilger, Bristol, 1988).

[26] V. F. Sears, Can. J. Phys. **44**, 1279 (1966).

[27] V. F. Sears, Can. J. Phys. **45**, 237 (1967).

[28] H. Taub, K. Carneiro, J. K. Kjems, L. Passell, and J. P. McTague, Phys. Rev. B **16**, 4451 (1977).

[29] M. T. Alkhafaji and A. D. Migone, Phys. Rev. **53**, 11152 (1996).

[30] F. Bach and H.-D. Lüdemann, Z. Naturforsch. **41**a, 963 (1986).

[31] D. Fuhrmann and Ch. Wöll, Surf. Sci. **377–379**, 544 (1997).